

Elastic magnetic electron scattering form factor in Ca-41 (M3Y fitting parameters consideration)

Raad A. Radhi and Firas Z. Majeed

Department of physics, Coll. of Science Baghdad Univ., Baghdad, Iraq

Abstract

Elastic magnetic electron scattering form factors in Ca-41 have been investigated. $1f_{7/2}$ subshell has been adopted as a model space with one neutron, and Millinar, Baymann and Zamick $1f_{7/2}$ model space effective interaction (F7MBZ) has been used as a model space effective interaction to generate the model space vectors for the M1, M3, M5, M7, and total form factors. Discarded space (core and higher configuration orbits) have been included through the first order perturbation theory to couple the particle-hole pair of excitation with $2\hbar\omega$ excitation energy in the calculation of the form factors and regarding the realistic interaction density dependence M3Y as a core polarization interaction with five sets of modern fitting parameters. Finally the theoretical calculations have been compared with the experimental data for such transition form factor.

Keywords

Elastic magnetic
electron scattering
M3Y fitting parameters
consideration

Article info

Received: Mar. 2010

Accepted: Apr. 2010

Published: Dec. 2010

دراسة عوامل التشكل الاستطارة الالكترونية للانتقالات المغناطيسية المرنة في نواة Ca^{41} (أعتبارات معاملات الضبط لتفاعلات البقية من نوع M3Y)

رعد عبد الكريم راضي و فراس زهير مجيد
قسم الفيزياء - كلية العلوم - جامعة بغداد/ بغداد-العراق

الخلاصة

تم حل معادلة بولتزمان للغازات النقية والمزيجات باستخدام التقريب ذي الحدين. استخدمت هذه الطريقة لحساب دالة توزيع طاقة الإلكترون ومعلمات الانتقال الالكتروني، حسب في مدى متغير من E/N
 $1 \times 10^{-17} V \text{ cm}^2 \leq E / N \leq 5 \times 10^{-15} V \text{ cm}^2$.

أظهرت تلك النتائج أن دالة توزيع طاقة الإلكترون لغاز CF_4 قريب من التوزيع الماكسويلي عند (1,2) تاوسند، بعد ذلك عندما تزداد E/N التوزيع يصبح غير ماكسويلي، سلوك معلمات الانتقال قريب من النتائج التجريبية في المصادر. سرعة انجراف الإلكترون في غاز رباعي فلوريد الكاربون كانت كبيره مقارنة مع بقية الغازات .

Introduction

Elastic electron scattering is the process that the scattered electron will leave the nucleus in its ground state and the major momentum is going to the whole nucleus, so the initial and the final single particle states have the same angular momentum

and energy for such transition. ^{41}Ca is the most important nuclear system because it gives starting point and a touch stone for microscopic description of nuclei and gives a chance to measure the radius of doubly closed nuclei in a stretched case ($j=1f_{7/2}$) neutron orbit through the elastic

magnetic electron scattering which may be defined as an elegant technique.

The elastic magnetic form factors of ^{41}Ca had been determined [1] with 180° electron scattering in the momentum-transfer range $0.9\text{-}2.0 \text{ fm}^{-1}$, an analysis of the data indicated that the amplitudes of the M3 and M5 multipoles were quenched by factors of 0.57 ± 0.16 and 0.68 ± 0.07 relative to the simple shell model. In contrast, the magnitude of the M7 form factors is in a good accord with this model. Including both the $2\hbar\omega$ particle-hole excitations and the Zuker-type multi-particle-multi-hole configuration mixing The elastic magnetic form factors of ^{17}O and ^{41}Ca were calculated with best agreement with the experimental data [2]

Radii determination for the $1d_{5/2}$ orbit in ^{17}O and the $1f_{7/2}$ orbit in ^{41}Ca which are within 2% less than those deduced from the magnetic electron scattering form factors had been carried out [3]. The displacement energies are also sensitive to the root mean square (r m s) radius of the valence orbits, and the Skyrme (SKX) interactions give radii for the $1d_{5/2}$ orbit in ^{17}O and the $1f_{7/2}$ orbit in ^{41}Ca which were within 2% less than those deduced from the magnetic electron scattering form factors.

The study on elastic magnetic form factors of exotic nuclei and the magnetic form factors of $^{15,17,19}\text{C}$, ^{23}O , ^{17}F , and $^{49,59}\text{Ca}$ calculated in the relativistic impulse approximation have found great differences in the form factors of the same nucleus with different configurations. Therefore, the elastic magnetic electron scattering can be used to determine the orbital of the last nucleon of odd-A exotic nuclei, their results can provide references for the electron scattering from exotic nuclei in the near future [4]. Through the first order perturbation theory, core and higher configuration orbits had been included with $2\hbar\omega$ excitation energy with the use of Elliotte fitting (M3Y-E) as a residual interaction to couple the particle-

hole pairs beside the contribution of model space $1f_{7/2}$ particle (single neutron) in order to calculate total and individual elastic magnetic electron scattering form factors[5], and the results are in a good agreements with the experimental data[2].

Theory

The reduced matrix element of the electron scattering operator T_A can be expressed as the sum of the product of the one-body density matrix elements (OBDM) $X_{i_f i_i}^A(\alpha, \beta)$ times the transition single - particle matrix elements (TSPM) $\langle \alpha || \hat{T}_A || \beta \rangle$ which is given by [6]:

$$\langle \Gamma_f || \hat{T}_A || \Gamma_i \rangle = \sum_{\alpha\beta} X_{i_f i_i}^A(\alpha, \beta) \langle \alpha || \hat{T}_A || \beta \rangle \dots\dots\dots(1)$$

α and β label single-particle orbits (isospin is included) for the shell model space. The states $|\Gamma_i\rangle$ and $|\Gamma_f\rangle$ are defined by the model space wave functions. Greek symbols are introduced to denote quantum numbers in coordinate space and isospace, i.e., $\Gamma_i \equiv J_i T_i$, $\Gamma_f \equiv J_f T_f$ and $A \equiv J T$. Regarding to the first-order perturbation theory (inclusion of discarded space), the single-particle matrix element of the one-body operator is given by [6],

$$\langle \alpha || \hat{T}_A || \beta \rangle = \langle \alpha || \hat{T}_A || \beta \rangle + \langle \alpha || \hat{T}_A \frac{Q}{E_i - H_0} V_{res} || \beta \rangle + \langle \alpha || V_{res} \frac{Q}{E_f - H_0} \hat{T}_A || \beta \rangle \dots\dots\dots(2)$$

The first term is the model space part (zero-order contribution). The second and third terms are the first-order contributions belonging to core and higher energy configurations (hec). The operator Q is the projection operator onto the space outside the model space.

The (hec) terms given in Eq. (2) are written as [6]

$$\sum_{\alpha_2 \alpha_2'} \frac{(-1)^{\beta+\alpha_2+\Gamma}}{e_{\alpha_2} - e_{\alpha_2'} - e_{\alpha_2} + e_{\alpha_2'}} (2\Gamma + 1) \begin{Bmatrix} \alpha & \beta \\ \alpha_2 & \alpha_2' \end{Bmatrix}$$

* $\langle \alpha \alpha_1 | V_{res} | \beta \alpha_2 \rangle \langle \alpha_2 || \hat{T}_A || \alpha_1 \rangle$
 + term with α_1 and α_2 exchanged
 with an over all minus sign(3)

where the index α_1 runs over particle states and α_2 over hole states and e_i is the single-particle energy, which is calculated according to [6] as,

$$e_{nlj} = (2n+l-\frac{1}{2})\hbar\omega + \begin{cases} -\frac{1}{2}(l+1)\langle f(r) \rangle_{nl} & \text{for } j=l-\frac{1}{2} \\ \frac{1}{2}l\langle f(r) \rangle_{nl} & \text{for } j=l+\frac{1}{2} \end{cases}$$

.....(4)

With

$$\langle f(r) \rangle_{nl} \approx -20A^{-2/3} \text{MeV}$$

$$\hbar\omega = 45A^{-1/3} - 25A^{-2/3} \text{(5)}$$

The single particle matrix elements reduced in both spin and isospin, are written in terms of the single-particle matrix elements reduced in spin only [6],

$$\langle \alpha || \hat{T}_A || \beta \rangle = \sqrt{\frac{2\Gamma+1}{2}} \sum_{\alpha_2} t_T(t_2) \langle \alpha_2 || \hat{T}_A || \alpha_1 \rangle$$

.....(6)

With

$$t_T(t_2) = \begin{cases} 1 & \text{for } T = 0 \\ (-1)^{\frac{1}{2}-t_2} & \text{for } T = 1 \end{cases}$$

.....(7)

When $t_2 = \frac{1}{2}$ for proton and $-1/2$ for neutron. Higher energy configurations are taken into consideration through 1p-1h excitations from the model space orbits into higher orbits. All excitations are considered with $2\hbar\omega$ excitations.

For the residual two-body interaction V_{res} , the M3Y interaction of Nakada. [7] is adopted. The form of the potential is defined in Eqs. (1) The parameters of 'Elliot' are used which are given in Table 2 of the mentioned reference. A transformation between *LS* and *jj* is used to get the relation between the two-body shell model matrix elements and the relative and the center of mass coordinates, using the harmonic oscillator radial wave functions with Talmi-Moshinsky transformation. Electron scattering form factors involving angular momentum *J* and momentum transfer *q*, between initial and final nuclear shell model states of spin $J_{i,f}$ and isospin $T_{i,f}$ are [6, 8],

$$|F_{J'}^{\eta}(q)|^2 = \frac{4\pi}{Z^2(2J_i+1)} \left| \sum_{T=0,1} (-1)^{T_f-T_i} \begin{Bmatrix} T_f & T & T_i \\ -T_{zf} & M_T & T_{zi} \end{Bmatrix} \langle \Gamma_f || T_{J,T}^{\eta}(q) || \Gamma_i \rangle \right|^2$$

$$\times |F_{c.m.}(q)|^2 \times |F_{f.s.}(q)|^2 \text{(8)}$$

Where V_{res} is expressed as follows [7, 10],

$$V_{res} = V_{12}^{(c)} + V_{12}^{(LS)} + V_{12}^{(TN)} + V_{12}^{(DD)}$$

.....(9)

$$V_{12}^{(c)} = \sum_n (t_n^{(SE)} P_{SE} + t_n^{(TE)} P_{TE} + t_n^{(SO)} P_{SO} + t_n^{(TO)} P_{TO}) f_n^{(c)}(r_{12})$$

$$V_{12}^{(LS)} = \sum_n (t_n^{(LSE)} P_{TE} + t_n^{(LSO)} P_{TO}) f_n^{(LS)}(r_{12}) L_{12} \cdot (\vec{S}_1 + \vec{S}_2)$$

$$V_{12}^{(TN)} = \sum_n (t_n^{(TNE)} P_{TE} + t_n^{(TNO)} P_{TO}) f_n^{(TN)}(r_{12}) r_{12}^2 S_{12}$$

$$V_{12}^{(DD)} = t^{(DD)} \{ (1-x^{(DD)}) P_{SE} + t_n^{(DD)} (1+x^{(DD)}) P_{TE} \} \delta^{(TN)}(r_{12})$$

.....(10)

where $t^{(SE)}$, $t^{(TE)}$, $t^{(SO)}$, $t^{(TO)}$ are fitting parameters on the singlet-even (SE), triplet-even (TE), singlet-odd (SO) and

triplet-odd (TO) two-particle states, respectively, while PSE, PTE, PSO and PTO are the projection operators on the singlet-even (SE), triplet-even (TE), singlet-odd (SO) and triplet-odd (TO) two-particle states, respectively, in central part (c), and $t^{(LSE)}$, $t^{(LSO)}$, are fitting parameters on the singlet-even (LSE), singlet-odd (LSO) two-particle states, respectively, in spin orbit part (LS), and $t^{(TNE)}$, $t^{(TNO)}$, are fitting parameters on the singlet-even (TNE), singlet-odd (TNO) two-particle states, respectively, in tensor part (TN), finally $t^{(DD)}$ and $x^{(DD)}$ are the density dependence parameters (DD).

Results and discussion

Through the first order perturbation theory and by the carefully selected residual interaction the core + higher configuration have been included with $2\hbar\omega$ excitation energy across the model space in order to predict the best values of modification for the total calculations and the effect of realistic interaction and their fitting parameters, so the comparison test of these five sets of fitting parameters for every case under study will reflect the important informations about each term in the core polarization realistic interaction beside the search on the most suitable one. Careful extrapolation of table (2) which shows the fitting parameters for each version of density versions which reflects its effects on the calculation of core polarization term and its effect on the total results, and it is clear that all of these five versions make the core parts deviated from the experimental data [2] in somehow reflecting finally in the deviation of the total form factors in comparison to the model space contribution as illustrated in figures (1, 2, 3, 4, 5), but in another hand and in the same figures the distributions of the multipolarities are seen to be have the same successive distributions along the momentum transfer ordinate for every version as same as that found in ref[5] where M3Y-Elliotte fitting had been used where some times written in an abbreviation as (M3Y-E), but it is so

important to compare between them in form factors multipolarities fashion as illustrated in figures (6, 7, 8, 9, 10) where the comparisons between total core polarization contributions in the elastic magnetic form factors of the five versions and for the multipolarities (M1, M3, M5, M7) respectively. It is clear that they are different from each other in their amplitudes, diffraction minima and momentum distribution and it is clear that the calculations of M3Y-P1 are differing from the four versions where they are not so clearly separated in their general behavior. Return to figures (1, 2, 3, 4, 5) the model space contributions are so closely coincide with the experimental data in amplitudes and momentum distribution so the conclusion is written as follows: “in elastic magnetic electron scattering form factors in ^{41}Ca the unique responsible is the model space contribution and there are no core polarization contributions or there are no core excitation had been happened (^{40}Ca is a hard core). Table (1) shows the values of one body density matrix elements for single neutron in $1f_{7/2}$ model space. dependent Michigan sum of three range Yukawa potential (DD-M3Y) or sometimes written in symbols belong to the so called Ried fitting as follows (M3Y-P1, M3Y-P2, M3Y-P3, M3Y-P4, M3Y-P5), this table shows the difference between these sets.

Table(1). The values of (OBDM) for elastic magnetic form factor in ^{41}Ca .

MJ	J _i	J _f	OBDM	OBDM
			($\Delta T=0$)	($\Delta T=1$)
M1	7/2	7/2	1	1
M3	7/2	7/2	1	1
M5	7/2	7/2	1	1
M7	7/2	7/2	1	1

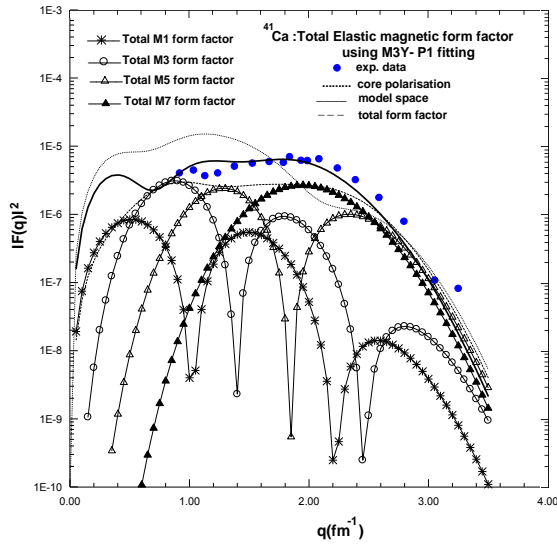


Fig. 1 Total elastic magnetic electron scattering form factors and total individual multipolarities (M1, M3, M5, M7) with M3Y-P1, exp data are taken from ref.[2].

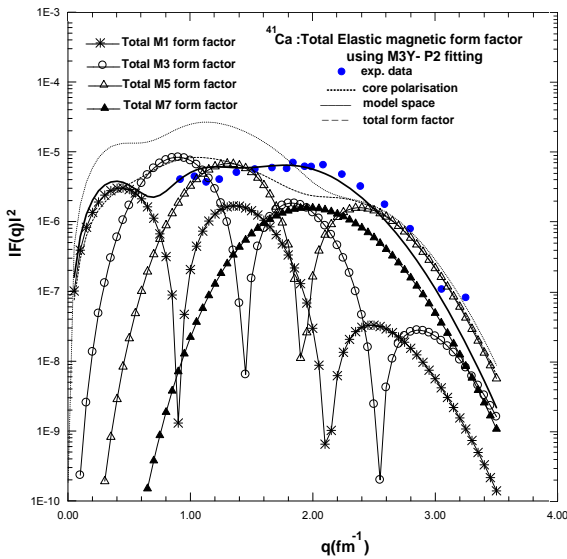


Fig. 2 Total elastic magnetic electron scattering form factors with and total individual multipolarities (M1, M3, M5, M7) M3Y-P2, exp data are taken from ref.[2].

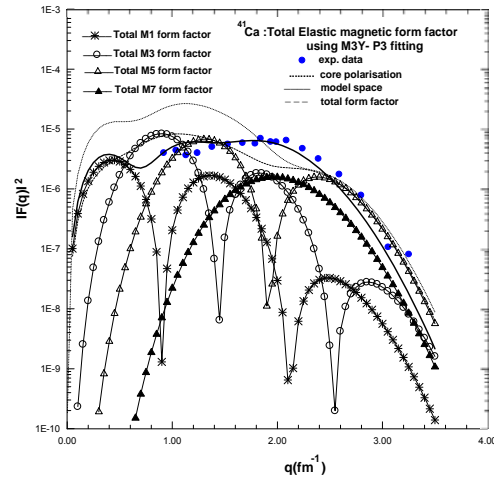


Fig. 3 Total elastic magnetic electron scattering form factors and total individual multipolarities (M1, M3, M5, M7) with M3Y-P3, exp data are taken from ref.[2].

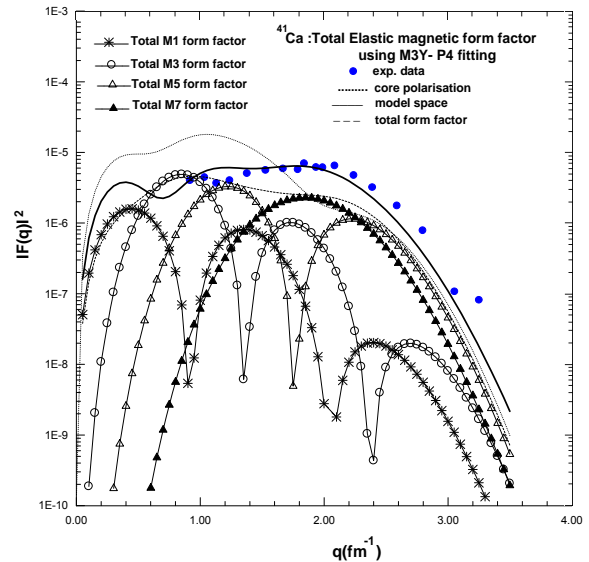


Fig. 4 Total elastic magnetic electron scattering form factors with and total individual multipolarities (M1, M3, M5, M7) M3Y-P4, exp data are taken from ref.[2].

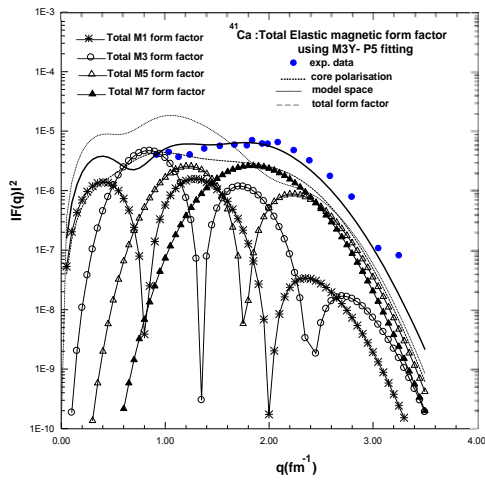


Fig. 5 Total elastic magnetic electron scattering form factors with and total individual multiplicities (M1, M3, M5, M7) M3Y-P5, exp data are taken from ref.[2].

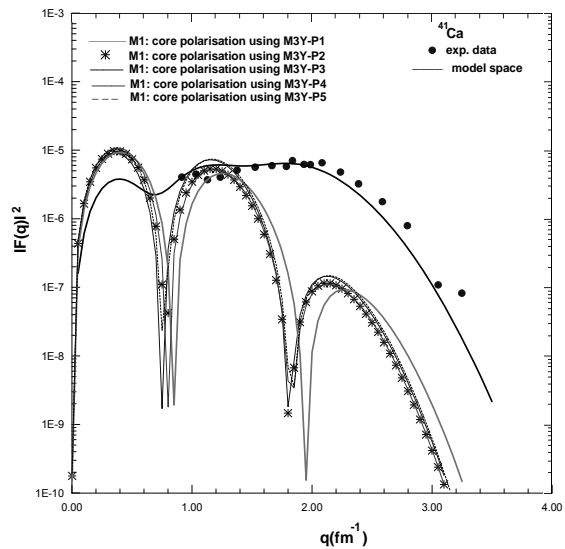


Fig. 7 Comparison between Total core polarization of elastic magnetic electron scattering M1 form factors with the use of five versions of M3Y interactions, exp data are taken from ref.[2].

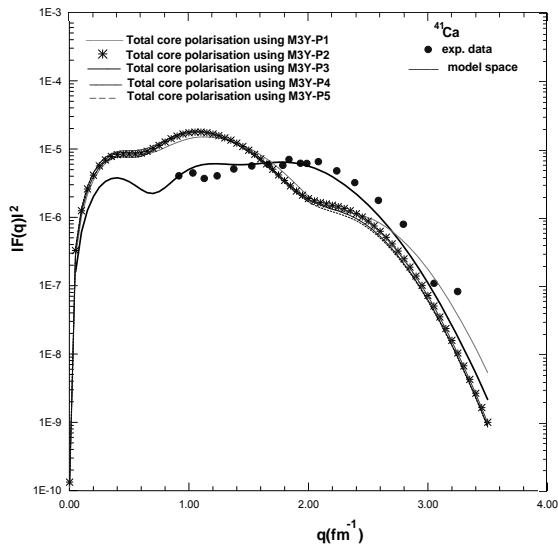


Fig. 6 Comparison between Total core polarization of elastic magnetic electron scattering form factors with the use of five versions of M3Y interactions, exp data are taken from ref.[2].

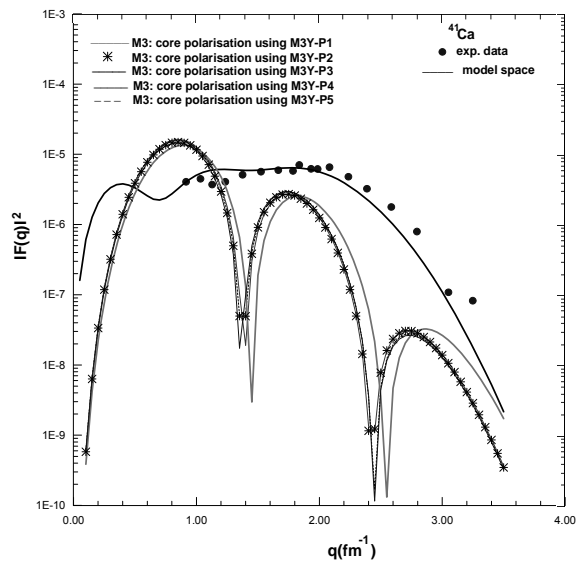


Fig. 8 Comparison between Total core polarization of elastic magnetic electron scattering M3 form factors with the use of five versions of M3Y interactions, exp data are taken from ref.[2].

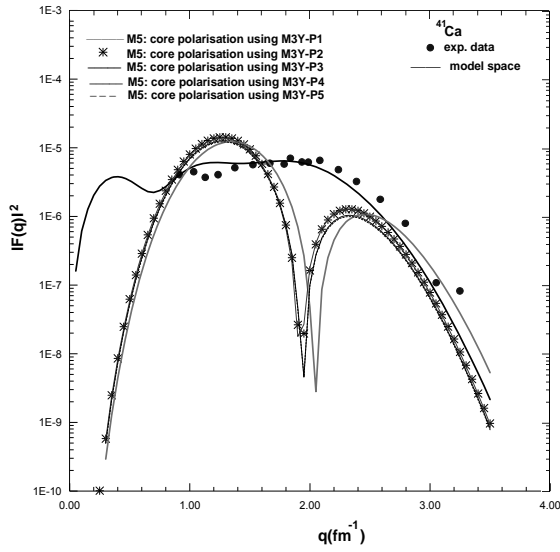


Fig. 9 Comparison between Total core polarization of elastic magnetic electron scattering M5 form factors with the use of five versions of M3Y interactions, exp data are taken from ref.[2].

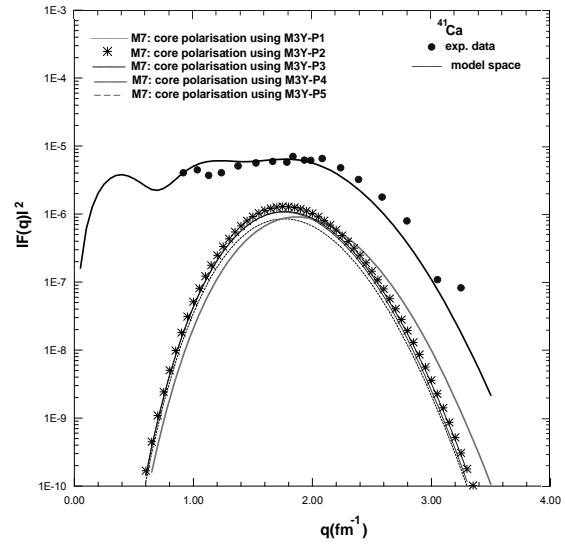


Fig. 10 Comparison between Total core polarization of elastic magnetic electron scattering M7 form factors with the use of five versions of M3Y interactions, exp data are taken from ref.[2].

Table (2). Shows the values of the best fit to the potential parameters [7].

Fitting Parameters	unit	M3Y-E*	M3Y-P0	M3Y-P1†	M3Y-P2	M3Y-P3	M3Y-P4	M3Y-P5
$R_1^{(C)}$	(fm)	0.25	0.25	0.25	0.25	0.25	0.25	0.25
$t_1^{(SB)}$	(MeV)	9958	11466.	8599.5	8027.	8027.	8027.	8027.
$t_1^{(FB)}$	(MeV)	11849	13967.	10475.2 5	6080.	7130.	5503.	5576.
$t_1^{(SO)}$	(MeV)	26941	-1418.	-1418.	-11900.	-1418.	-12000.	-1418.
$t_1^{(T)}$	(MeV)	0.0	11345.	11345.	3800.	11345.	3700.	11345.
$R_2^{(C)}$	(fm)	0.40	0.40	0.40	0.40	0.40	0.40	0.40
$t_2^{(SB)}$	(MeV)	-3105	-3556.	-3556.	-2880.	-2637.	-2637.	-2650.
$t_2^{(FB)}$	(MeV)	-3761	-4594.	-4594.	-4266.	-4594.	-4183.	-4170.
$t_2^{(SO)}$	(MeV)	-2777	950.	950.	2730.	950.	4500.	2880.
$t_2^{(T)}$	(MeV)	0.0	-1900.	-1900.	-780.	-1900.	-1000.	-1780.
$R_3^{(C)}$	(fm)	1.414	1.414	1.414	1.414	1.414	1.414	1.414
$t_3^{(SB)}$	(MeV)	-10.463	-10.463	-10.463	-10.463	-10.46 3	-10.46 3	-10.463
$t_3^{(FB)}$	(MeV)	-10.463	-10.463	-10.463	-10.463	-10.46 3	-10.46 3	-10.463
$t_3^{(SO)}$	(MeV)	31.389	31.389	31.389	31.389	31.389	31.389	31.389
$t_3^{(T)}$	(MeV)	3.488	3.488	3.488	3.488	3.488	3.488	3.488
$R_1^{(SB)}$	(fm)	0.25	0.25	0.25	0.25	0.25	0.25	0.25
$t_1^{(SSB)}$	(MeV)	0.0	-5101.	-9181.8	-9181.8	-10712.1	-8671.7	-11222.2
$t_1^{(SSO)}$	(MeV)	-2672	-1897.	-3414.6	-3414.6	-3983.7	-3224.9	-4173.4
$R_2^{(SB)}$	(fm)	0.40	0.40	0.40	0.40	0.40	0.40	0.40
$t_2^{(SSB)}$	(MeV)	-813.0	-337.	-606.6	-606.6	-707.7	-572.9	-741.4

Table (2). Shows the values of the best fit to the potential parameters [7]

Parameters	unit	M3Y-E*	M3Y-P0†	M3Y-P1	M3Y-P2	M3Y-P3	M3Y-P4	M3Y-P5
$t_1^{(M3Y)}$	(MeV)	-2672	-1897.	-3414.6	-3414.6	-3983.7	-3224.9	-4173.4
$R_1^{(M3Y)}$	(fm)	0.40	0.40	0.40	0.40	0.40	0.40	0.40
$t_2^{(M3Y)}$	(MeV)	-813.0	-337.	-606.6	-606.6	-707.7	-572.9	-741.4
$t_3^{(M3Y)}$	(MeV)	-620.0	-632.	-1137.6	-1137.6	-1327.2	-1074.4	-1390.4
$R_2^{(M3Y)}$	(fm)	1.414	1.414	1.414	1.414	1.414	1.414	1.414
$t_4^{(M3Y)}$	(MeV)	0.0	0.0	0.0	0.0	0.0	0.0	0.0
$t_5^{(M3Y)}$	(MeV)	0.0	0.0	0.0	0.0	0.0	0.0	0.0
$R_3^{(FN)}$	(fm)	0.4	0.4	0.4	0.4	0.4	0.4	0.4
$t_1^{(FN)}$	(MeV fm ⁻²)	0.0	-1096.	-131.52	-131.52	-1096.	0.0	-1096.
$t_2^{(FN)}$	(MeV fm ⁻²)	0.0	244.	29.28	29.28	244	0.0	244.
$R_4^{(FN)}$	(fm)	0.70	0.70	0.70	0.70	0.70	0.70	0.70
$t_3^{(FN)}$	(MeV fm ⁻²)	-171.7	-30.9	-3.708	-3.708	-30.9	0.0	-30.9
$t_4^{(FN)}$	(MeV fm ⁻²)	283.0	15.6	1.872	1.872	15.6	0.0	15.6
$R_5^{(FN)}$	(fm)	1.414	1.414	1.414	1.414	1.414	1.414	1.414
$t_5^{(FN)}$	(MeV fm ⁻²)	-78.03	0.0	0.0	0.0	0.0	0.0	0.0
$t_6^{(FN)}$	(MeV fm ⁻²)	13.62	0.0	0.0	0.0	0.0	0.0	0.0
$t_{DD}^{(SE)}$	(MeV fm)	0.0	0.0	1092	181.	220.	248.	126.
$t_{DD}^{(FE)}$	(MeV fm)	0.0	0.0	1331	1139.	1198.	1142.	1147.

*Ref.[11], †Ref[10].

Acknowledgements

The authors would like to express their thanks to Professor B.A. Brown of the National superconducting cyclotron laboratory, Michigan State University for providing them the computer code OXBASH.

References

- [1] H. Baghaei, A. Cichocki, J. B. Flanz, M. Frodyma, B. Frois, Y. Han, R. S. Hicks, J. Martino, R. A. Miskimen, C. N. Papanicolas, G. A. Peterson, S. Platchkov, S. Raman, S. H. Rokni and T. Suzuki, Phys. Rev. C42, 2358 (1990).
- [2] C. Zheng, D. W. L. Sprung, and L. Zamick, Nucl. Phys. A540, 57 (1992).
- [3] T. Suzuki, H. Sagawa and A. Arima, Nucl. Phys. A536, 141 (1992).
- [4] T. Dong, Z. Ren, and Y. Guo, Phys. Rev. C76, 054602 (2007).
F. Z. Majeed, Dissertation of Ph degree in physics (2009).
- [5] P. J. Brussaard and P. W. M. Glademans, "Shell-model Application in Nuclear Spectroscopy", (North-Holland Publishing Company, Amsterdam (1977)).
- [6] H. Nakada, Phys. Rev. C 78, 054301 (2008).
- [7] T. W. Donnelly and I. Sick, Rev-Mod. Phys. 56, 461 (1984).
- [8] J. D. McCullen, B. F. Bayman and L. Zamick, Phys. Rev. 134, B515 (1963).
- [9] H. Nakada, Phys. Rev. C68. 014316 (2003).
- [10] T. P. Elliott and B. H. Flowers, Proc. Roy. Soc. A242, 57 (1959).